GEOCHEMISTRY

Origin of potassic postcollisional volcanic rocks in young, shallow, blueschist-rich lithosphere

Yu Wang[1,2,3]*, Stephen F. Foley[3,4], Stephan Buhre[5], Jeremie Soldner[1,2], Yigang Xu[1,2,6]

Potassium-rich volcanism occurring throughout the Alpine-Himalayan belt from Spain to Tibet is characterized by unusually high Th/La ratios, for which several hypotheses have brought no convincing solution. Here, we combine geochemical datasets from potassic postcollisional volcanic rocks and lawsonite blueschists to explain the high Th/La. Source regions of the volcanic melts consist of imbricated packages of blueschist facies mélanges and depleted peridotites, constituting a new mantle lithosphere formed only 20 to 50 million years earlier during the accretionary convergence of small continental blocks and oceans. This takes place entirely at shallow depths (<80 km) without any deep subduction of continental materials. High Th/La in potassic rocks may indicate shallow sources in accretionary settings even where later obscured by continental collision as in Tibet. This mechanism is consistent with a temporal trend in Th/La in potassic postcollisional magmas: The high Th/La signature first becomes prominent in the Phanerozoic, when blueschists became widespread.

INTRODUCTION

Potassic volcanism commonly occurs in the late stages of orogenesis—the process of collision of plates—between a long-lasting period of subduction and the end of postcollisional collapse. The transformation of an arc system into a collisional regime is usually accompanied by volcanism that geochemically resembles the older arc lavas and yet has important additional ingredients derived from the continental lithosphere. The syn-collisional episode evolves into a postcollisional phase during which volcanism may be extremely variable due to a combination of slab detachment, delamination, slab rollback, and extension, and each of these processes may involve different sources and melting regimes (*1*, *2*). These processes are reflected in the geochemistry of the erupted orogenic magmas, which represent the end result of complex, multistage processes. Furthermore, in some regions such as Tibet, where massive continental collision occurred later, the tectonic regime in which potassic volcanism occurs may be obfuscated by later tectonic processes. Here, the potassic volcanism may have originated in an environment similar to the modern eastern Mediterranean, which predating the continental collision (*3*).

The tectonic regime that triggered widespread orogenic volcanism in the Alpine-Himalayan chain is controversial (*4*, *5*). There is now abundant evidence from trace elements and isotopes for the involvement of continental material in the source (*5*, *6*), but the style and mechanism of this crustal involvement remain unclear. Two competing scenarios invoke (i) direct melting of continental crust during deep intercontinental subduction (*7*) and (ii) delamination of heavily metasomatized mantle lithosphere into the convecting mantle where melting of its most fusible parts occurs (*8*, *9*). However, direct evidence to distinguish between these two models has been lacking.

The Th/La ratio has been used to assess whether certain chemical features shared by arc magmas and continental crust are induced by subduction processes or are derived from recycled subducted sediment (*10*). This study suggested that in normal circumstances, the Th/La ratio of mantle-derived magmas should be relatively constant and no greater than 0.5. However, postcollisional lamproites of the "Tethyan-realm," which later developed into the Alpine-Himalayan orogenic belt (AHOB), were reported to have high Th/La ratios of up to 2.2 (*8*). Given their exceptional enrichment in potassium and other strongly incompatible elements, lamproites have been considered the optimal probe to characterize strongly metasomatized mantle to constrain the source of the Alpine-Himalayan orogenic magmatism (*3*, *11*). The unusual geochemical signature of extremely high Th/La coupled with relatively low Sm/La is not restricted to lamproites in the AHOB, as described by Tommasini *et al.* (*8*), but also occurs in many other K-rich volcanic rocks in the same belt (Fig. 1). Two main mechanisms have been put forward to explain this anomalously high Th/La: (i) preferential uptake of La relative to Th in mafic minerals during direct melting of continental crust (*10*, *12*) and (ii) melting of mélanges that include lawsonite/zoisite-bearing blueschists accreted to the colliding continental plates (*8*, *9*, *13*, *14*).

Here, we propose a comprehensive model that is a variant of the second hypothesis. This model explains the source regions of the AHOB potassic volcanic rocks as consisting of blueschist facies mélanges (including oceanic crust, oceanic, and continental sediments) imbricated together with extremely depleted forearc peridotites. Together, these make up a mantle lithosphere that was newly formed during the convergence of small continental blocks and oceans. The imbrication process took place entirely at shallow depths (<80 km) and did not require any deep subduction of continental materials. Lawsonite blueschists provide notable new petrological and geochemical evidence to explain the Th/La fractionation widely seen in AHOB K-rich lavas.

RESULTS

Geological background: Tavşanlı zone, Turkey

During the Cretaceous, the Alpine-Himalayan chain was dominated by the convergence of continents that eliminated the northern

[1]State Key Laboratory of Isotope Geochemistry, Guangzhou Institute of Geochemistry, Chinese Academy of Sciences, Guangzhou 510640, China. [2]CAS Center for Excellence in Deep Earth Science, Guangzhou 510640, China. [3]ARC Centre of Excellence for Core to Crust Fluid Systems, Department of Earth and Environmental Sciences, Macquarie University, Sydney, NSW 2109, Australia. [4]Research School of Earth Sciences, Australian National University, Canberra, ACT 2601, Australia. [5]Institute for Geosciences, University of Mainz, J.J. Becher-Weg 21, Mainz 55099, Germany. [6]School of Earth and Planetary Sciences, University of Chinese Academy of Sciences, Beijing 100049, China.
*Corresponding author. Email: wangyu@gig.ac.cn

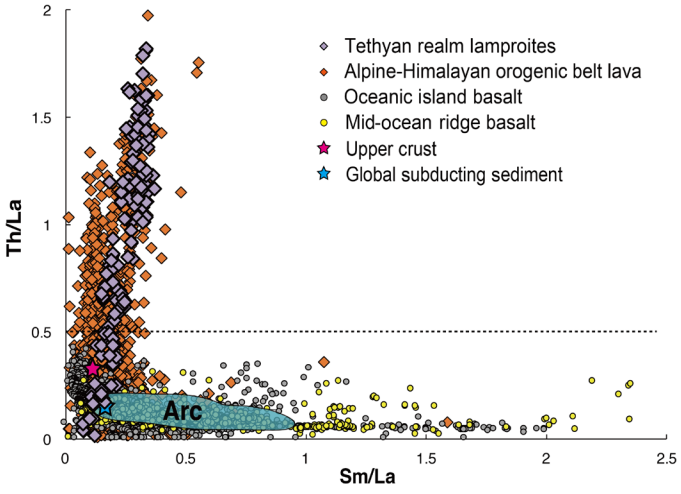

Fig. 1. Sm/La versus Th/La in rocks with different origins. The diagram includes Tethyan realm lamproites (purple diamonds) (*8*), AHOB lavas (orange diamonds; data file S1),oceanic island basalt (GEOROC database, http://georoc.mpch-mainz.gwdg.de/georoc), mid-ocean ridge basalt (MORB) (GEOROC database, http://georoc.mpch-mainz.gwdg.de/georoc), upper crust, and global subducting sediment (*54*). "Arc" field, magmas related to slab-derived mantle metasomatism [(*8*) and the references therein]. Values of Th/La > 0.5 (dotted line) are considered anomalous and characteristic of AHOB lavas.

branch of the Neotethyan Ocean. This convergence resulted in the growth of accretionary prisms in many regions, including the Anatolian sector of the belt. The Tavşanlı zone in north-eastern Anatolia extends ca. 250 km east to west and 50 to 60 km north to south, lying south of the major Izmir-Ankara-Erzincan suture (fig. S1B) (*15*). It represents an ophiolitic mélange thrust sheet, comprising mixed rocks that are interpreted as a subducted accretionary prism formed during the tectonic closure of a section of the Neotethyan Ocean. The Tavşanlı mélange was accreted beneath northern Anatolia in the form of several continental slivers and numerous oceanic island arcs and comprises metamorphosed basic volcanic rocks, cherts, shales, marbles, and clastic sequences derived from the continental margin. Pressure-temperature (P-T) estimates for the metamorphism of the Tavşanlı zone are ~300° to 500°C, 12 to 24 kbar (*16*). The lawsonite blueschist data used here are from a coherent blueschist unit, the Orhaneli sequence that consists mainly of three major formations of metasedimentary rocks; the samples were collected from the upper Devlez formation [mostly metabasite (fig. S1, C and D) (*17*)]. The depositional age of the blueschist metaclastics is Mesozoic, and the age of blueschist metamorphism, based on Rb/Sr phengite dating, is Campanian [~80 Ma, (*18*)], whereas more recent studies of Lu-Hf dating yielded a lawsonite eclogite age of 91.1 Ma, a garnet-lawsonite blueschist age of 83.3 Ma (*19*) and lawsonite blueschist facies ages between 90 and 86 Ma (*20*). Moreover, a new in situ $^{40}Ar/^{39}Ar$ dating study on phengite showed much wider age range for metamorphism of ~20 Ma for these rocks (*21*).

Mineral parageneses

Six lawsonite blueschists were selected from a large collection of samples from the Tavşanlı zone (*17*). The mineral assemblage is mainly lawsonite + sodic amphibole + phengite + chlorite + titanite + apatite ± aragonite ± quartz ± relict igneous pyroxene ± Mn-rich garnet and opaque phases (hematite, galena, and pyrite). Euhedral prismatic lawsonite grains up to 500 μm are present in all samples. Lawsonite is intergrown with acicular or tabular sodic amphibole crystals, phengite, chlorite, fine-grained titanite, and apatite. Large zones of quartz are observed in two samples (10tav05 and 10tav07), the latter of which also contains subhedral Mn-rich garnet grains. Unaltered lawsonite porphyroblasts occur in all samples, containing very small titanite, glaucophane, and aragonite inclusions.

Whole-rock geochemistry and isotopic constraints

Whole rock Sr, Nd, and Pb isotopes and incompatible element concentrations show considerable differences in the extent of isotope and trace element enrichment (*17*). Three lawsonite blueschists have low concentrations of K, Th, U, and rare earth element (REE), coupled with slight and variably radiogenic $^{87}Sr/^{86}Sr$ but radiogenic $^{143}Nd/^{144}Nd$ similar to mid-ocean ridge basalt (MORB). These samples also have the most unradiogenic $^{206}Pb/^{204}Pb$, $^{207}Pb/^{204}Pb$, and $^{208}Pb/^{204}Pb$ compositions, plotting within the depleted MORB mantle field and implying MORB-like oceanic crust protoliths. The other three samples are more enriched in K, and especially in Th, U, and light REE (LREE), and show variably radiogenic $^{87}Sr/^{86}Sr$ and mostly unradiogenic $^{143}Nd/^{144}Nd$. The most unradiogenic $^{143}Nd/^{144}Nd$ indicates the presence of an enriched, probably continental crust-like, component. These samples have more radiogenic $^{206}Pb/^{204}Pb$, $^{207}Pb/^{204}Pb$, and $^{208}Pb/^{204}Pb$ than the MORB-like samples, although they mostly plot within the mantle array.

Lawsonite compositions

Calcium aluminosilicate phases such as epidote group minerals and lawsonite may contain significant amounts of trace elements, with lawsonite known to be a potentially important repository for Th, Sr, U, and REE (*17*, *22*–*25*). The concentrations of Th, large-ion lithophile element (LILE), and LREE in lawsonite were found to be highly variable within individual Tavşanlı samples. This strong heterogeneity in trace element concentrations is not due to zoning or contamination from inclusions and probably results from differing origins of the lawsonite (*23*, *24*). Sample 10tav07 is distinctive in showing a positive correlation between extremely high Th/La (up to 1.1) and relatively high Sm/La ratios. This is consistent with several previous studies, in which high Th/La (up to 4.88) has been found in lawsonites from nearby Sivrihisar (Fig. 2) (*23*). Mass balance calculations indicate that ~40% of Th is held in lawsonite (25 modal %) in sample 10tav07 (*17*), underscoring the significance of lawsonite in governing the Th budget of blueschists. This enrichment is coupled with REE fractionation in lawsonite and low $^{87}Sr/^{86}Sr$ and $^{143}Nd/^{144}Nd$ in the whole rock, which suggests the involvement of an enriched component similar to continental crust. In contrast, the MORB-like samples exhibit low Th/La but markedly high Sm/La ratios (Fig. 2).

Minor amounts of inclusions of minerals such as monazite and epidote group minerals, especially allanite, have the potential to falsify the trace element concentrations of lawsonite markedly (*12*). This has been discounted for the data used here by thoroughly investigating lawsonites by three-dimensional confocal micro-Raman spectroscopic mapping: only glaucophane, quartz, and titanite were found, which cannot greatly affect trace element concentrations in lawsonite (*17*).

Fingerprinting the geochemistry of Alpine-Himalayan orogenic magmatism

Previous studies of the isotopic and chemical heterogeneities of mantle-derived K-rich lavas from the AHOB, mostly of lamproitic

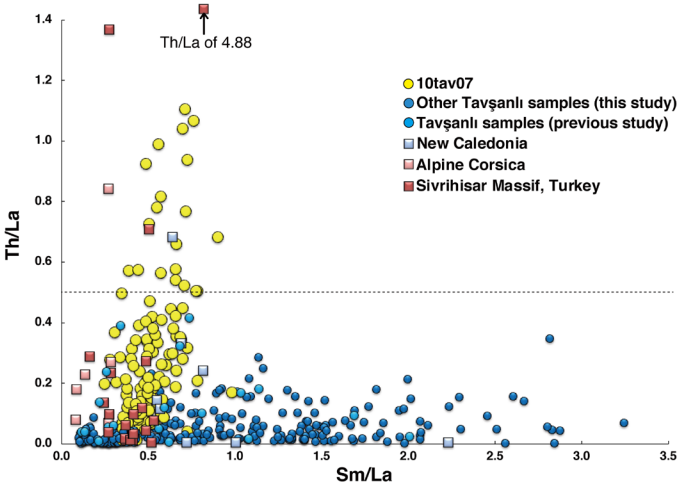

Fig. 2. Sm/La versus Th/La in natural lawsonites. Sm/La and Th/La of lawsonite in sample 10tav07 correlates positively, as in the AHOB lavas in Fig. 1, accentuated by the analyses from nearby Sivrihisar (*23*). New Caledonia data from Spandler *et al.* (*22*), Alpine Corsica data from Vitale Brovarone *et al.* (*24*), and previous Tavşanlı data from Fornash *et al.* (*55*) and Fornash and Whitney (*56*). For lawsonite data from this study, see data file S2.

affinity, mandate the involvement of three components in the source: (i) a continental crustal component (*8*, *9*, *26*), indicated by incompatible-element enrichment, elevated $^{87}Sr/^{86}Sr$, $^{207}Pb/^{204}Pb$, $^{187}Os/^{188}Os$, and low $^{143}Nd/^{144}Nd$ and $^{176}Hf/^{177}Hf$ ratios. These isotopic signatures complement high Th/La, Th/Yb, Th/Nb, predominantly high Hf/Sm, and low Ce/Pb and Nb/U ratios; (ii) a strongly depleted peridotite component identified by refractory Cr-spinel, highly magnesian olivine, and relatively low whole-rock FeO abundances (*9*, *13*); (iii) the enigmatic high Th/La component, which is coupled with high Sm/La (Fig. 1) (*8*, *9*, *14*, *17*).

Here, we examine these fingerprints further using a robust geochemical database for AHOB volcanic rocks (data file S1), which includes lamproites, coeval basalts, shoshonites, and andesites, occurring throughout the AHOB. Data were selected on the basis of their close association with the Alpine-Himalayan orogen and postcollisional geodynamics, spanning the area from Morocco, Spain, Mediterranean, and India to Tibet (fig. S1A). Na-alkaline asthenosphere–derived lavas associated with the circum-Mediterranean anorogenic Cenozoic igneous activity (*27*) are excluded. The database is screened to exclude lavas with less than 3 weight % (wt %) MgO, thus avoiding crustal contamination and eliminating the most highly fractionated magmas (*5*). We emphasize that the use of a higher MgO screen, as is commonly done for mantle-derived melts, would implicitly assume a peridotite source, which is inappropriate for a region in which continental crust and melts derived from it are known to play a major role.

Several important observations can be summarized from the database. Generally, they show a trace element pattern typical for volcanic rocks of island arcs and continental margins, which is attributed to a major role of volatiles in element transfer from the subducted slab to the mantle wedge. There are, however, substantial variations in several key geochemical parameters. We tentatively subdivide them into two major groups using K_2O/Na_2O as a geochemical discriminator: (i) low-K lavas or "normal" arc lavas ($K_2O/Na_2O < 1$; e.g., South Aegean active volcanic arc), with potassium contents that are low in the most primitive members of the suite but increase with fractionation; (ii) high-K lavas ($K_2O/Na_2O > 1$), which have high K_2O content also in the most Mg-rich samples (Fig. 3, A and B). Despite some overlap between the two populations on some plots, high-K lavas are systematically more enriched in Th, with many showing elevated Th/La and Th/Yb (Fig. 3, C and E). Moreover, they have more radiogenic strontium and less radiogenic neodymium isotopes (Fig. 3D), interpreted to suggest that their source contains a terrigenous crustal component. The isotopic and chemical differences between low- and high-K lavas indicate the existence of distinct mantle sources.

DISCUSSION

The crust-like signature and Th enrichment identified previously in lamproites may be extended to the entire K-rich group of AHOB lavas. Because Th enrichment in the high-K lavas (high Th/La and Th/Yb) rises as K_2O and $^{87}Sr/^{86}Sr_{(i)}$ increase and as $^{143}Nd/^{144}Nd_{(i)}$ decreases, we may conclude that recycled continental crust plays a significant role in the source. However, neither continental and oceanic crust nor their derivatives show enrichment in Th and elevated Th/La and Th/Yb ratios (*8*, *10*), implying that this signature does not simply arise by crustal recycling. In other words, the high Th/La signature must be newly created during the orogenic cycle without losing the isotopic affinities.

Lawsonite blueschists in the source of potassic magmas

Th/La ratios of both the blueschist whole rocks and the lawsonites yield heterogeneous values, whereby the most elevated Th/La ratios are in the terrigenous samples with the continent-derived geochemical component characterized by unradiogenic Nd isotopes (*17*). The most enriched blueschist sample (10tav07) plots at values typical for continental crust, implying that blueschist from mélange may play a substantial role in the origin of the AHOB lavas, providing the geochemical ingredients responsible for the continental crust-like signature and elevated Th/La ratios. Lawsonites from this sample show the extremely high Th/La values as well as a positive correlation between Th/La and Sm/La ratios (Fig. 2), a similar correlation to that seen in the orogenic lavas (Fig. 1). This contrasts with melts of the upper crust, which fail to appreciably fractionate Th from La at any degree of melting (*14*). This supports the hypothesis that lawsonite blueschist in mélanges can host the high Th/La signature in the postcollisional potassic volcanic rocks of the Alpine-Himalayan belt. The high Th/La ratios of lawsonites can be conveyed to the AHOB lavas by a series of progressive geological processes, not only by prograde metamorphic recrystallization into new mineral phases, which would redistribute trace elements differently (*22*).

Allanite, monazite, and epidote group minerals are known to host considerable amounts of Th and LREE (*28*, *29*), so these minerals are often assumed to be the most likely candidates to account for the elevated Th/La ratios. Although a few experimental studies have reported that allanite is able to fractionate Th from La (*12*, *30*), existing data on natural minerals show that they are not likely to be responsible for the high Th/La ratios, because none of these minerals fractionate Th from La as effectively as lawsonite (all have Th/La < 0.5; fig. S2). Moreover, even if allanite does have the potential to account for the high Th/La, it is also a common lawsonite blueschist facies mineral (*22*, *23*, *31*) and so does not contradict our proposal of the significance of blueschist facies mélange in conveying the Th/La characteristics to AHOB lavas.

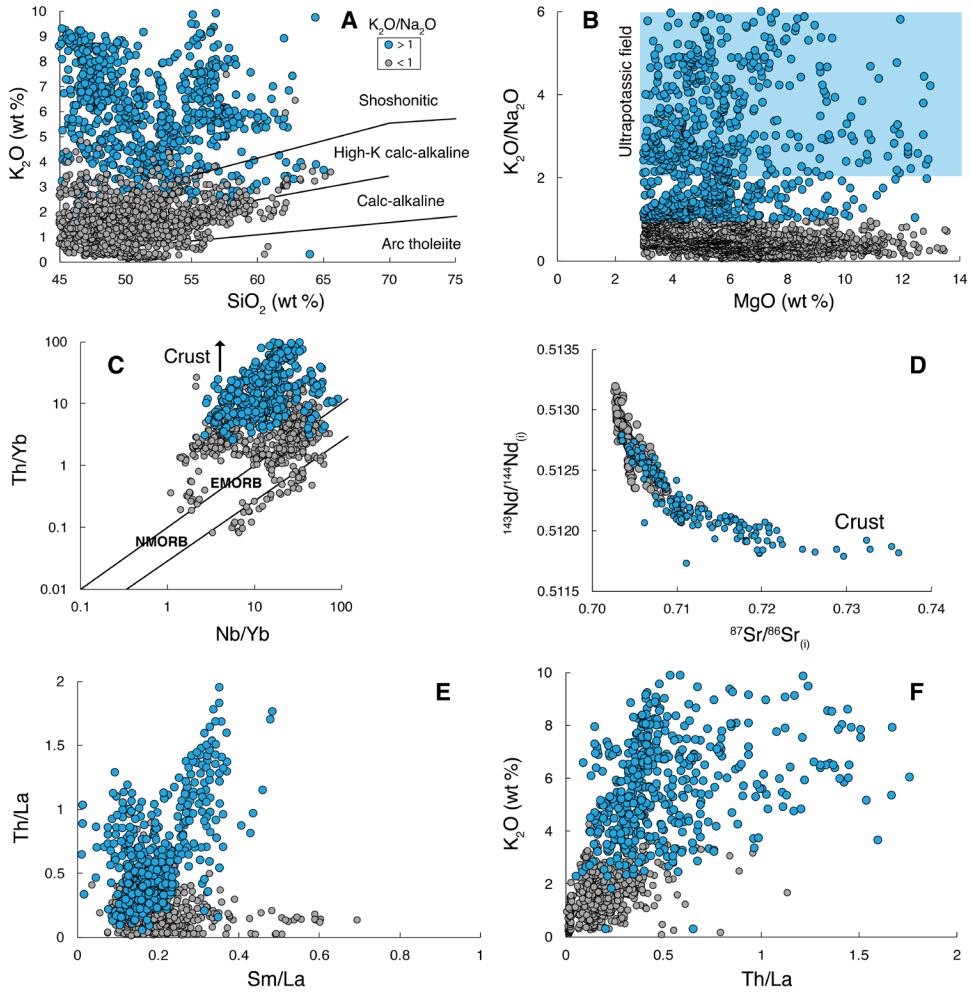

Fig. 3. Geochemical affinities of AHOB lavas with MgO (wt %) > 3%. (**A**) SiO_2 (wt %) versus K_2O (wt %); (**B**) MgO (wt %) versus K_2O/Na_2O ratio; (**C**) Nb/Yb versus Th/Yb; (**D**) initial Nd-Sr isotope compositions; (**E**) Sm/La versus Th/La ratios; and (**F**) Th/La versus K_2O (wt %). For AHOB data, see data file S1.

A key question that needs to be addressed pertains to the petrological mechanism of blueschist involvement in the origin of the melts, particularly why they are potassium rich and have unusually high Th/La ratios. It is clear from our data that only the terrigenous blueschists can provide the coupled elevated Th/La and crust-like trace element signature to the source of the AHOB lavas (*17*). Because phlogopite is often assumed to be an essential contributor to strongly potassic magmatism (*32*), it is easy to generalize the origin of K-rich magmatism as being derived from deep mantle levels. However, reaction experiments between quartz phyllite and depleted peridotite produce potassic, silicic melts without residual phlogopite (*33*), indicating that the assumption of phlogopite in the source may not apply in all cases. Although our samples are not very phengite-rich, we envisage that some portions of the blueschist facies mélange are extremely enriched in potassium and trace elements typical for the continental crust [e.g., (*34*)]. Experimental studies of the melting of mélange show that melt compositions depend critically on the exact rock type among the heterogeneous mélange that melts. Some indicate that granodioritic to tonalitic melts would be produced (*35*), whereas melting of chlorite-omphacite–dominated rocks produces melts with the major and trace element characteristics of postcollisional alkaline lavas (*36*). However, because of the lack of terrigenous lawsonite blueschist in the starting material, their study did not produce melts with elevated Th/La ratios.

Multistage evolution of elevated Th/La in Alpine-Himalayan volcanic rocks

The history of the collision, lithosphere formation, and remelting in the AHOB might be exclusively a shallow level process in which mélange recycling takes place within the relatively cold fore-arc region at low pressure (path a in Fig. 4A) (*14*). This contrasts with conventional deep Andean-style subduction (path c in Fig. 4A) in which a succession of additional reactions at higher pressures would dilute the Th/La signature, as shown in the quantitatively modeled figure (Fig. 4D).

Lawsonite blueschists may have an array of trace element ratios depending on their origins: terrigenous blueschists will contain the high Th/La feature while others (e.g., MORB-like blueschists) do not (*17*). As tectonic imbrication occurs, a variety of rock types can be stored for considerable time in the blueschist facies in the newly formed lithosphere, unlike Andean-style subduction in which metamorphism would progress relatively quickly to the eclogite facies (path c in Fig. 4, A and B). Blueschists are initially stable in the

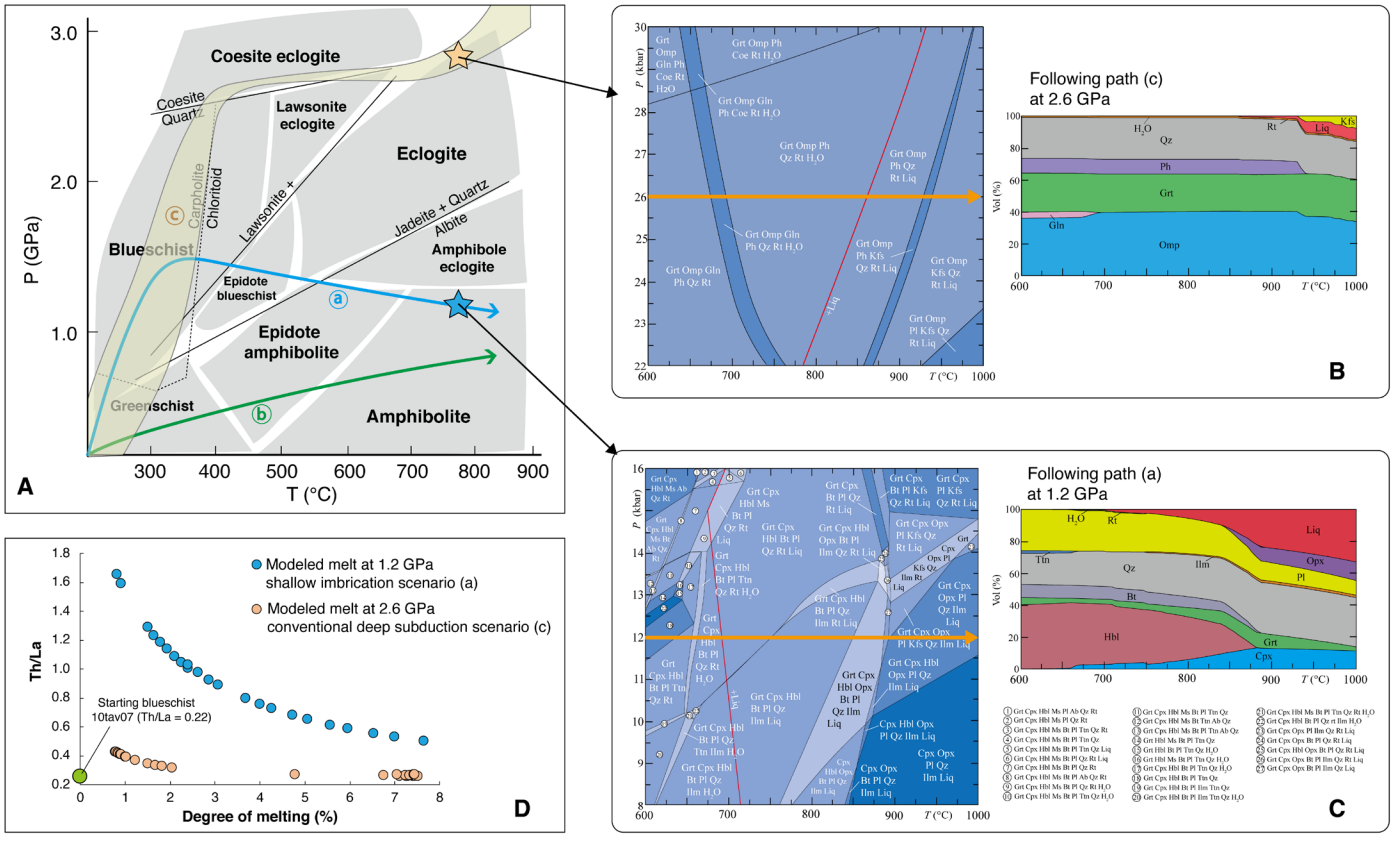

Fig. 4. Deep subduction versus shallow imbrication. (**A**) Three contrasting prograde P-T-t paths for (a) shallow subduction and tectonic imbrication discussed for the Alpine-Himalayan belt (blue line), (b) normal regional (orogenic) metamorphic scenario [after Çetinkaplan *et al.* (*57*) and Plunder *et al.* (*16*)] (green line), and (c) conventional deep Andean-style subduction [beige shaded field after Syracuse *et al.* (*58*)]. During subduction, path a reaches blueschist facies, and tectonic imbrication may store abundant blueschists in the lithosphere. This material is now removed from the subduction environment and is isolated from further movements. During postcollisional processes, these rocks slowly heat up path a and move slowly from blueschist, through epidote amphibolite to upper amphibolite facies. In contrast, path b follows a path from greenschist to epidote amphibolite then to amphibolite but does not pass through the blueschist facies. (**B** and **C**) Full pressure-temperature (P-T) pseudosection diagrams for the Tavşanlı blueschist 10tav07 at 600° to 1000°C, 0.8 to 1.6 GPa and 2.2 to 3.0 GPa following paths a and c in (A), respectively. Also shown are calculated modal proportions for melting along apparent pressure of 1.2 and 2.6 GPa. Plots of modal proportions versus temperature (also known as modebox diagrams) illustrate the changing abundance of phases, modeled along linear pressure of 1.2 and 2.6 GPa (orange arrow lines). (**D**) Comparison between modeled Th/La ratios for melts produced at 1.2 GPa (shallow imbrication scenario) and melts produced at 2.6 GPa (conventional deep subduction scenario) at given degree of melting. Starting Th/La in blueschist 10tav07 is 0.22 (*17*), many blueschists have higher ratios. Note the notable difference of Th/La ratios between the two types of modeled melts. Grt, garnet; Omp, omphacite; Gln, glaucophane; Ph, phengite; Coe, coesite; Qz, quartz; Rt, rutile; Kfs, K-feldspar; Pl, plagioclase; Liq, melt; Cpx, clinopyroxene; Opx, orthopyroxene; Hbl, hornblende; Ttn, titanite; Bt, biotite; Ilm, ilmenite; Ms, muscovite; Ab, albite.

newly formed lithosphere but will slowly heat up during postcollisional orogenic collapse. Because the thickened crust slowly relaxes and thins in postcollisional conditions (*37*), it takes 10 to 30 Ma for the lower block to achieve thermal equilibrium (*38*), which agrees well with the timing of postcollisional volcanism, which first occurs after this period. However, the P-T-t path consists mostly of heating with a slight reduction in pressure due to extension and to erosion of the continent above it during postcollisional relaxation. The effect is to slowly move from the blueschist to epidote amphibolite and then the upper part of the amphibolite facies, which may be garnet-bearing (path a in Fig. 4, A and C) (*34*, *39*). Eventually, the lawsonite blueschists will transform in subsolidus metamorphic conditions, and the lawsonite will break down. When it does, a fluid will be lost, and because Th is less soluble in hydrous fluids than La (*40*), more La is transported away in the fluid, leaving the residue (regardless of its mineralogy) with an enhanced Th/La ratio. Melting first occurs in the amphibolite facies. Existing partition coefficients for amphibole (*41*) and feldspar (*42*, *43*) show $D_{Th}/D_{La} < 1$, meaning that when melting occurs in the amphibolite facies, the residue will hold back more La than Th, and Th/La ratio in the residue will be increased further, which is confirmed by the quantitative model (Fig. 4D). It should be noted here that many blueschist samples have higher Th/La than the sample 10tav07 used in the model shown in Fig. 4D, so that melts of these will retain high Th/La to higher degrees of melting than in Fig. 4D.

In the case of the most K-rich volcanics, source-rocks will contain considerable biotite and/or muscovite in addition to amphibole and alkali feldspar, which will enhance the potassium contents of later melts. Feldspar will remain in the residue together with amphibole or clinopyroxene, all of which will retain Na, increasing the K/Na of coexisting melts. The melts produced from these sources will have high Th/La but also intermediate to high SiO_2, meaning that

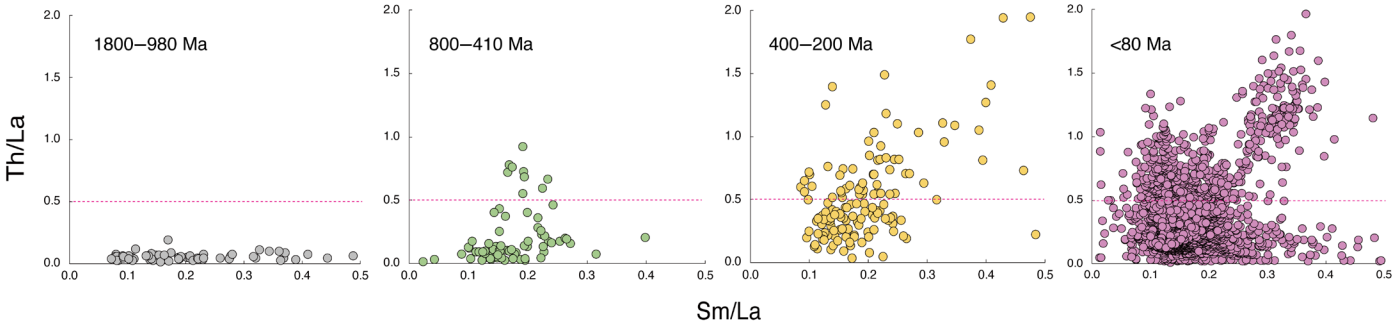

Fig. 5. Temporal variation in Sm/La versus Th/La of K-rich orogenic volcanics through time. From <80 Ma (Alpine-Himalayan orogen), 200 to 400 Ma (South China, Central Asian, and Variscan orogens), and 410 to 800 Ma (Appalachian, Caledonide, Brasiliano, and Pan-African orogens) to 980 to 1800 Ma (Grenvillian and Svecofennian orogens) (see data file S3 for data sources; this database is screened to exclude magmas with $K_2O/Na_2O < 1$ and MgO < 3 wt %). Note there is a clear secular trend of increasing Th/La ratio through time where no elevated Th/La present for Grenvillian and Svecofennian times.

they contribute a relatively high-SiO_2 end-member to the cocktail of source components. This is consistent with the positive correlation of Th/La with SiO_2 contents in the postcollisional volcanics.

The uniquely high Th/La signature in AHOB volcanic rocks may, therefore, result from three consecutive processes that progressively increase the Th/La ratio: (i) initial incorporation of high Th/La in lawsonite; (iii) loss of a hydrous fluid (breakdown of lawsonite); and (iii) melting of originally continental crustal rocks in the amphibolite facies. It should be noted that amphibolites need not be restricted to metabasites; a metapelite may have distinct mineralogy, containing quartz, orthoclase, muscovite, biotite, garnet, etc. (*44*, *45*). Melts of this amphibolite would be potassic and could give rise to the potassium enrichment seen widely in AHOB volcanic rocks.

The P-T-t path usually considered for the stability of many accessory minerals (such as allanite, monazite, and epidote) is different to that in this new geodynamic scenario. A normal regional (orogenic) metamorphic field gradient moves through greenschist to amphibolite and not via the blueschist facies (path b in Fig. 4A), so that the prograde mineral assemblages differ. For an Andean subduction (path c in Fig. 4A), blueschists cannot escape the fate of being transformed to eclogite as the slab proceeds to deeper levels. Therefore, experiments that simply displace a continental crustal rock to high PT conditions and analyze trace elements in accessory minerals do not account for the correct history of mineral assemblage changes relevant to shallow accretionary processes.

Temporal trends of Th/La in orogenic magmatism

The oldest glaucophane schists preserved on Earth are Neoproterozoic and lawsonite-bearing blueschists appear much later (~Ordovician), so that blueschist-facies metamorphism is practically restricted to the Phanerozoic (*46*). If lawsonite blueschists are essential for the production of K-rich orogenic magmas with high Th/La ratios, then a logical consequence of our model is that K-rich volcanic rocks in older orogenic belts should show progressively lower and more confined Th/La ratios as we go back in time. To test this prediction, we plot published Th/La data in K-rich orogenic magmas from geochronologically diverse orogens in Fig. 5. As we go back in time from <80 Ma through 200 to 400 Ma and from 410 to 800 Ma through 980 to 1800 Ma, a secular trend from high to low Th/La ratio is indeed clearly visible, with no elevated Th/La present for Grenvillian and Svecofennian times (980 to 1800 Ma; Fig. 5). This further justifies the shallow subduction model and the significance of lawsonite blueschists in the production of K-rich orogenic magmas with high Th/La ratios.

Implications and outlook

Convergence along the Alpine-Himalayan belt varied in style, involving accretion of small continental slivers and numerous oceanic island arcs in the west, culminating in the world's most comprehensive continental collision in the east. Most of the convergence between Gondwana and Eurasia since the Cretaceous has been accommodated by nappe stacking and lithospheric slab underthrusting. In many regions, oceanic subduction waned during the Cretaceous, shortly after which postcollisional tectonics dominated during a period of large-scale extension (*47*). Magmatism is closely related to tectonics: It postdates the final accretionary events that formed the Alpine-Himalayan chain, with the most voluminous and widely distributed episode(s) beginning in the late Cretaceous. Magma genesis is controlled by a combination of rollback of the underthrusting lithospheric slab that initiated postcollisional extension and collapse of the orogenic belts, coupled with the initiation and progression of slab tear (*5*).

Complex geodynamic settings are the key to activating and melting a variety of mantle and crustal sources: Slab rollback triggers the suction of hot convecting mantle toward shallow levels in the mantle wedge, and hot, fresh asthenospheric mantle may also penetrate through slab tears, causing melting of previously enriched domains in the lithospheric mantle. In this process, rollback plays a specific role in the fate of lawsonite, which exerts control of critical trace element ratios in relatively shallow subduction zone conditions along cold geotherms (450° to 650°C and 2 to 3 GPa) (*23*). As the subducting slab descends into the mantle, continental sediments experience prograde metamorphism during which trace elements are redistributed from precursor minerals (most likely epidote group minerals or Mn-garnet) to lawsonite, glaucophane, jadeite, and white mica. Lawsonite takes up much of the Th, Sr, and REE, whereas Nb and Ta are preferentially incorporated in rutile and titanite, Zr and Hf in zircon, LILE in phengite, and heavy REE in garnet. Lawsonites that grow in locally different components of a lithologically heterogeneous subduction mélange inherit the geochemical characteristics of their oceanic or continental protoliths. It is now uncertain whether the high Th/La signature is derived from mixed continental and oceanic sedimentary protoliths or from metasomatic reactions caused by fluids transporting more La than Th from continental blocks when they infiltrate oceanic mélange.

The Alpine-Himalayan orogenic volcanics thus owe their unusual trace element geochemistry, especially the extremely high Th/La ratios, to the involvement of lawsonite blueschists in the source region. Their incorporation in newly formed lower lithosphere and the 30- to 50-Ma time span before magmatism are consistent with petrological-thermomechanical modeling (*48*). The extremely high Th/La signature in lawsonite can be transferred to the postcollisional lavas by multistage accumulation in an entirely shallow level process (Fig. 4), consistent with P-T estimates for the Tavşanlı zone of ~300° to 500°C, 12 to 24 kbar, which correspond to lithospheric depths of 40 to 80 km. This highlights an unrecognized bias in past studies, which have unconsciously supposed deep, Andean-style subduction where the slab proceeds to lower mantle depths.

These scenarios are specifically relevant to accretionary orogens in which the limited size of small subducting oceanic slabs and continental blocks prevents deep subduction processes from dominating. For places where the accretionary stages could be largely obscured by later major collision, e.g., in Tibet (*3*, *49*), the proposed scenario is especially applicable and could provide additional geodynamic perspectives complementary to existing knowledge. Although this tectonic scenario has been recognized in Turkey and Tibet because the continental sediment signature is observed in the Pb isotope compositions of post-collisional lavas (*5*, *8*), we predict that there will often be abundant oceanic sediments integrated into the lithosphere. All these components are reactivated and melted during mechanical relaxation millions of years after the collision. These processes are significant for arcs and orogenic magmatism on the modern Earth but will be particularly pertinent to the late Archean, during which crustal formation by the amalgamation of arcs may have been widespread (*50*).

MATERIALS AND METHODS

Thermodynamic modeling

To constrain melt crystallization at high-pressure and low-pressure conditions, P-T pseudosection calculations have been applied for a representative terrigenous blueschist composition (sample 10tav07) (*17*). Phase equilibria were calculated using PerpleX version 6.8.1 software package (*51*) with the upgraded thermodynamic database DS6.22 from Holland and Powell (*52*). Pseudosections for composition of blueschist 10tav07 were calculated in the $MnO—Na_2O—CaO—K_2O—FeO—MgO—Al_2O_3—SiO_2—H_2O—TiO_2—O$ (MnNCKFMASHTO) system. The activity-solution models used were taken from literature and tabulated in data file S4. The composition of CaO of blueschist 10tav07 has been adjusted using the Rock Maker software (*53*) to account for the presence of 6 mode% of apatite that has not been included in the pseudosection calculations. The O content has been determined using calculated T–X(O) pseudosection at 1.2 GPa to constrain the oxidation state able to predict stability of the rock mineral assemblage. The H_2O contents at high- and low-pressure conditions have been determined using two calculated T–X(H_2O) pseudosections to constrain the minimum content in H_2O necessary for the rock to cross the solidus after potential subsolidus water loss at 2.6 and 1.2 GPa, respectively. The results for high-pressure melting are shown in a P-T pseudosection calculated with H_2O = 1.53 mol % and O = 0.17 mol % between 2.2 and 2.6 GPa and 600° and 1000°C. The results for low-pressure melting are shown in a P-T pseudosection calculated with H_2O = 3.94 mol % and O = 0.17 mol % between 8 and 16 GPa and 600° and 1000°C. Assemblage fields are labeled with stable phases while pure phases include quartz, rutile, sphene (titanite), and aqueous fluid (H_2O). The thick labeled black line represents the liquid-in reaction. The depth of shading reflects increasing variance of phase assemblage fields. The bulk-rock composition used for pseudosection calculations at high- and low-pressure conditions is given in data file S4. The software and data files used to calculate the pseudosections can be downloaded from http://www.perplex.ethz.ch.

Trace-element modeling

For Th/La ratio modeling (Fig. 4D), we used blueschist sample 10tav07 as a starting composition (Th/La = 0.22) (*17*) and the calculated abundance of phases at 600° to 1000°C, 1.2 and 2.6 GPa, respectively, at various melt fractions (Fig. 4, B and C, and data file S4). Mineral/melt partition coefficients (*D*) were taken from the literature and tabulated in data file S4.

SUPPLEMENTARY MATERIALS

Supplementary material for this article is available at http://advances.sciencemag.org/cgi/content/full/7/29/eabc0291/DC1

REFERENCES AND NOTES

1. M. J. R. Wortel, W. Spakman, Subduction and slab detachment in the Mediterranean-Carpathian region. *Science* **290**, 1910–1917 (2000).
2. M. Lustrino, S. Duggen, C. L. Rosenberg, The Central-Western Mediterranean: Anomalous igneous activity in an anomalous collisional tectonic setting. *Earth Sci. Rev.* **104**, 1–40 (2011).
3. Z. Guo, M. Wilson, M. Zhang, Z. Cheng, L. Zhang, Post-collisional ultrapotassic mafic magmatism in South Tibet: Products of partial melting of pyroxenite in the mantle wedge induced by roll-back and delamination of the subducted Indian Continental Lithosphere slab. *J. Petrol.* **56**, 1365–1406 (2015).
4. S.-L. Chung, M.-F. Chu, Y. Zhang, Y. Xie, C.-H. Lo, T.-Y. Lee, C.-Y. Lan, X. Li, Q. Zhang, Y. Wang, Tibetan tectonic evolution inferred from spatial and temporal variations in post-collisional magmatism. *Earth Sci. Rev.* **68**, 173–196 (2005).
5. D. Prelević, C. Akal, S. F. Foley, R. L. Romer, A. Stracke, P. Van Den Bogaard, Ultrapotassic mafic rocks as geochemical proxies for post-collisional dynamics of orogenic lithospheric mantle: The case of southwestern Anatolia, Turkey. *J. Petrol.* **53**, 1019–1055 (2012).
6. D. Liu, Z. Zhao, D.-C. Zhu, Y. Niu, D. J. DePaolo, T. M. Harrison, X. Mo, G. Dong, S. Zhou, C. Sun, Z. Zhang, J. Liu, Postcollisional potassic and ultrapotassic rocks in southern Tibet: Mantle and crustal origins in response to India–Asia collision and convergence. *Geochim. Cosmochim. Acta* **143**, 207–231 (2014).
7. N. O. Arnaud, P. Vidal, P. Tapponnier, P. Matte, W. M. Deng, The high K_2O volcanism of northwestern Tibet: Geochemistry and tectonic implications. *Earth Planet. Sci. Lett.* **111**, 351–367 (1992).
8. S. Tommasini, R. Avanzinelli, S. Conticelli, The Th/La and Sm/La conundrum of the Tethyan realm lamproites. *Earth Planet. Sci. Lett.* **301**, 469–478 (2011).
9. D. Prelevic, D. E. Jacob, S. F. Foley, Recycling plus: A new recipe for the formation of Alpine-Himalayan orogenic mantle lithosphere. *Earth Planet. Sci. Lett.* **362**, 187–197 (2013).
10. T. Plank, Constraints from Thorium/Lanthanum on Sediment Recycling at Subduction Zones and the Evolution of the Continents. *J. Petrol.* **46**, 921–944 (2005).
11. A. Peccerillo, Multiple mantle metasomatism in central-southern Italy: Geochemical effects, timing and geodynamic implications. *Geology* **27**, 315–318 (1999).
12. J. Hermann, D. Rubatto, Accessory phase control on the trace element signature of sediment melts in subduction zones. *Chem. Geol.* **265**, 512–526 (2009).
13. D. Prelević, S. F. Foley, Accretion of arc-oceanic lithospheric mantle in the Mediterranean: Evidence from extremely high-Mg olivines and Cr-rich spinel inclusions in lamproites. *Earth Planet. Sci. Lett.* **256**, 120–135 (2007).
14. Y. Wang, D. Prelević, S. Buhre, S. F. Foley, Constraints on the sources of post-collisional K-rich magmatism: The roles of continental clastic sediments and terrigenous blueschists. *Chem. Geol.* **455**, 192–207 (2017a).
15. A. M. C. Şengör, Y. Yilmaz, Tethyan evolution of Turkey: A plate tectonic approach. *Tectonophysics* **75**, 181–241 (1981).
16. A. Plunder, P. Agard, C. Chopin, A. Pourteau, A. I. Okay, Accretion, underplating and exhumation along a subduction interface: From subduction initiation to continental subduction (Tavşanlı zone, W. Turkey). *Lithos* **226**, 233–254 (2015).
17. Y. Wang, D. Prelević, S. F. Foley, Geochemical characteristics of lawsonite blueschists in tectonic mélange from the Tavşanlı zone, Turkey: Potential constraints on the origin of Mediterranean potassium-rich magmatism. *Am. Mineral.* **104**, 724–743 (2019).

18. S. Sherlock, S. Kelley, S. Inger, N. Harris, A. Okay, ^{40}Ar-^{39}Ar and Rb-Sr geochronology of high-pressure metamorphism and exhumation history of the Tavşanlı zone, NW Turkey. *Contrib. Mineral. Petrol.* **137**, 46–58 (1999).
19. S. R. Mulcahy, J. D. Vervoort, P. R. Renne, Dating subduction-zone metamorphism with combined garnet and lawsonite Lu-Hf geochronology. *J. Metam. Geol.* **32**, 515–533 (2014).
20. A. Pourteau, E. E. Scherer, S. Schorn, R. Bast, A. Schmidt, L. Ebert, Thermal evolution of an ancient subduction interface revealed by Lu–Hf garnet geochronology, Halilbağı complex (Anatolia). *Geosci. Front.* **10**, 127–148 (2019).
21. K. F. Fornash, M. A. Cosca, D. L. Whitney, Tracking the timing of subduction and exhumation using ^{40}Ar/^{39}Ar phengite ages in blueschist- and eclogite-facies rocks (Sivrihisar, Turkey). *Contrib. Mineral. Petrol.* **171**, 67 (2016).
22. C. Spandler, J. Hermann, R. Arculus, J. Mavrogenes, Redistribution of trace elements during prograde metamorphism from lawsonite blueschist to eclogite facies; implications for deep subduction-zone processes. *Contrib. Mineral. Petrol.* **146**, 205–222 (2003).
23. L. A. J. Martin, J. Hermann, L. Gauthiez-Putallaz, D. L. Whitney, A. Vitale Brovarone, K. F. Fornash, N. J. Evans, Lawsonite geochemistry and stability–implication for trace element and water cycles in subduction zones. *J. Metam. Geol.* **32**, 455–478 (2014).
24. A. Vitale Brovarone, O. Alard, O. Beyssac, L. Martin, M. Picatto, Lawsonite metasomatism and trace element recycling in subduction zones. *J. Metam. Geol.* 489–514 (2014).
25. D. L. Whitney, K. F. Fornash, P. Kang, E. D. Ghent, L. Martin, A. I. Okay, A. V. Brovarone, Lawsonite composition and zoning as tracers of subduction processes: A global review. *Lithos* **370–371**, 105636 (2020).
26. S. Conticelli, A. Peccerillo, Petrology and geochemistry of potassic and ultrapotassic volcanism in central Italy: Petrogenesis and inferences on the evolution of the mantle sources. *Lithos* **28**, 221–240 (1992).
27. M. Lustrino, M. Wilson, The circum-Mediterranean anorogenic Cenozoic igneous province. *Earth Sci. Rev.* **81**, 1–65 (2007).
28. R. Gieré, S. S. Sorensen, Allanite and Other REE-Rich Epidote-Group Minerals. *Rev. Mineral. Geochem.* **56**, 431–493 (2004).
29. A. S. Stepanov, J. Hermann, D. Rubatto, R. P. Rapp, Experimental study of monazite/melt partitioning with implications for the REE, Th and U geochemistry of crustal rocks. *Chem. Geol.* **300–301**, 200–220 (2012).
30. K. Klimm, J. D. Blundy, T. H. Green, Trace element partitioning and accessory phase saturation during H_2O-saturated melting of basalt with implications for subduction zone chemical fluxes. *J. Petrol.* **49**, 523–553 (2008).
31. D. Frei, A. Liebscher, G. Franz, P. Dulski, Trace element geochemistry of epidote minerals. *Rev. Mineral. Geochem.* **56**, 553–605 (2004).
32. S. F. Foley, An experimental study of olivine lamproite: First results from the diamond stability field. *Geochim. Cosmochim. Acta* **57**, 483–489 (1993).
33. Y. Wang, S. F. Foley, D. Prelević, Potassium-rich magmatism from a phlogopite-free source. *Geology* **45**, 467–470 (2017b).
34. A. I. Okay, D. L. Whitney, Blueschists, eclogites, ophiolites and suture zones in northwest Turkey: A review and a field excursion guide. *Ofioliti* **35**, 131–171 (2010).
35. A. Castro, T. Gerya, A. García-Casco, C. Fernández, J. Díaz-Alvarado, I. Moreno-Ventas, I. Löw, Melting relations of MORB–sediment melanges in underplated mantle wedge plumes; implications for the origin of cordilleran-type batholiths. *J. Petrol.* **51**, 1267–1295 (2010).
36. A. M. Cruz-Uribe, H. R. Marschall, G. A. Gaetani, V. Le Roux, Generation of alkaline magmas in subduction zones by partial melting of mélange diapirs—An experimental study. *Geology* **46**, 343–346 (2018).
37. C. Jaupart, J. C. Mareschal, Post-orogenic thermal evolution of newborn Archean continents. *Earth Planet. Sci. Lett.* **432**, 36–45 (2015).
38. P. England, P. L. Fort, P. Molnar, A. Pêcher, Heat sources for Tertiary metamorphism and anatexis in the Annapurna-Manaslu region central Nepal. *J. Geophys. Res. Solid Earth* **97**, 2107–2128 (1992).
39. A. I. Okay, N. B. W. Harris, S. P. Kelley, Exhumation of blueschists along a Tethyan suture in northwest Turkey. *Tectonophysics* **285**, 275–299 (1998).
40. L. A. J. Martin, B. J. Wood, S. Turner, T. Rushmer, Experimental measurements of trace element partitioning between lawsonite, zoisite and fluid and their implication for the composition of arc magmas. *J. Petrol.* **52**, 1049–1075 (2011).
41. M. Tiepolo, R. Oberti, A. Zanetti, R. Vannucci, S. F. Foley, Trace-element partitioning between amphibole and silicate melt. *Rev. Mineral. Geochem.* **67**, 417–452 (2007).
42. M. Ren, Partitioning of Sr, Ba, Rb, Y, and LREE between alkali feldspar and peraluminous silicic magma. *Am. Mineral.* **89**, 1290–1303 (2004).
43. J. H. Bédard, Trace element partitioning in plagioclase feldspar. *Geochim. Cosmochim. Acta* **70**, 3717–3742 (2006).
44. A. E. Wright, Amphibolite facies, in *Petrology* (Encyclopedia of Earth Science, Springer US, Boston, MA, 1990), pp. 12–16.
45. R. W. White, R. Powell, T. J. B. Holland, T. E. Johnson, E. C. R. Green, New mineral activity–composition relations for thermodynamic calculations in metapelitic systems. *J. Metam. Geol.* **32**, 261–286 (2014).
46. M. Brown, Metamorphic conditions in orogenic belts: A record of secular change. *Int. Geol. Rev.* **49**, 193–234 (2007).
47. Y.-F. Zheng, Convergent plate boundaries and accretionary wedges, in *Encyclopedia of Geology (Second Edition)*, D. Alderton, S. A. Elias, Eds. (Academic Press, Oxford, 2021), pp. 770–787.
48. C. M. Gonzalez, W. Gorczyk, T. V. Gerya, Decarbonation of subducting slabs: Insight from petrological–thermomechanical modeling. *Gondw. Res.* **36**, 314–332 (2015).
49. F. Cai, L. Ding, R. J. Leary, H. Wang, Q. Xu, L. Zhang, Y. Yue, Tectonostratigraphy and provenance of an accretionary complex within the Yarlung–Zangpo suture zone, southern Tibet: Insights into subduction–accretion processes in the Neo-Tethys. *Tectonophysics* **574–575**, 181–192 (2012).
50. K. C. Condie, Origin and early growth rate of continents. *Precambrian Res.* **32**, 261–278 (1986).
51. J. A. D. Connolly, Computation of phase equilibria by linear programming: A tool for geodynamic modeling and its application to subduction zone decarbonation. *Earth Planet. Sci. Lett.* **236**, 524–541 (2005).
52. T. J. B. Holland, R. Powell, An improved and extended internally consistent thermodynamic dataset for phases of petrological interest, involving a new equation of state for solids. *J. Metam. Geol.* **29**, 333–383 (2011).
53. S. H. Büttner, Rock Maker: An MS Excel™ spreadsheet for the calculation of rock compositions from proportional whole rock analyses, mineral compositions, and modal abundance. *Miner. Petrol.* **104**, 129–135 (2012).
54. T. Plank, C. H. Langmuir, The chemical composition of subducting sediment and its consequences for the crust and mantle. *Chem. Geol.* **145**, 325–394 (1998).
55. K. F. Fornash, D. L. Whitney, N. C. A. Seaton, Lawsonite composition and zoning as an archive of metamorphic processes in subduction zones. *Geosphere* **15**, 24–46 (2018).
56. K. F. Fornash, D. L. Whitney, Lawsonite-rich layers as records of fluid and element mobility in subducted crust (Sivrihisar Massif, Turkey). *Chem. Geol.* **533**, 119356 (2020).
57. M. Çetinkaplan, O. Candan, R. Oberhänsli, R. Bousquet, Pressure–temperature evolution of lawsonite eclogite in Sivrihisar; Tavşanlı Zone–Turkey. *Lithos* **104**, 12–32 (2008).
58. E. M. Syracuse, P. E. van Keken, G. A. Abers, The global range of subduction zone thermal models. *Phys. Earth Planet. In.* **183**, 73–90 (2010).
59. S. Maruyama, J. G. Liou, M. Terabayashi, Blueschists and eclogites of the World and their exhumation. *Int. Geol. Rev.* **38**, 485–594 (1996).
60. J. Hermann, Allanite: Thorium and light rare earth element carrier in subducted crust. *Chem. Geol.* **192**, 289–306 (2002).
61. B. A. Wing, J. M. Ferry, T. M. Harrison, Prograde destruction and formation of monazite and allanite during contact and regional metamorphism of pelites: Petrology and geochronology. *Contrib. Mineral. Petrol.* **145**, 228–250 (2003).
62. R. Gieré, D. Rumble, D. Günther, J. Connolly, M. J. Caddick, Correlation of growth and breakdown of major and accessory minerals in metapelites from Campolungo, Central Alps. *J. Petrol.* **52**, 2293–2334 (2011).

Acknowledgments: We thank T. Johnson and R. White for helpful discussions about thermodynamic equilibrium in the Tavşanlı zone and C. Akal for informative work in the field. We appreciate D. Prelević and S. Tommasini for insightful comments on an early version of this manuscript. O. Jagoutz and S. Mulcahy are greatly thanked for constructive reviews, and the editorial support of C.-T. Lee is appreciated. **Funding:** This work was supported by the Strategic Priority Research Program (B) of Chinese Academy of Sciences (grant no. XDB18000000), National Natural Science Foundation of China (grant no. 41773055), the ARC Centre of Excellence for Core to Crust Fluid Systems (CCFS), and the Youth Innovation Promotion Association of the Chinese Academy of Sciences (2020348). S.F.F. is funded by ARC grant FL180100134. J.S. is supported by the CAS President's International Fellowship Initiative for Postdoctoral Researchers (grant no. 2021PC0013). **Author contributions:** Y.W. and S.F.F. designed the project and wrote the paper. Y.W. carried out most of the laboratory work and data processing and performed SEM, electronic microprobe, LA-ICP-MS, and Raman spectrometry analyses. S.B. participated in SEM and electron microprobe work. J.S. helped in conducting PerpleX calculation. Y.W., S.F., and Y.X. jointly interpreted data. **Competing interests:** The authors declare that they have no competing interests. **Data and materials availability:** All data needed to evaluate the conclusions in the paper are present in the paper and/or the Supplementary Materials. Additional data related to this paper may be requested from the authors.

Submitted 2 April 2020
Accepted 28 May 2021
Published 14 July 2021
10.1126/sciadv.abc0291

Citation: Y. Wang, S. F. Foley, S. Buhre, J. Soldner, Y. Xu, Origin of potassic postcollisional volcanic rocks in young, shallow, blueschist-rich lithosphere. *Sci. Adv.* **7**, eabc0291 (2021).

ScienceAdvances

Origin of potassic postcollisional volcanic rocks in young, shallow, blueschist-rich lithosphere

Yu WangStephen F. FoleyStephan BuhreJeremie SoldnerYigang Xu

Sci. Adv., 7 (29), eabc0291. • DOI: 10.1126/sciadv.abc0291

Science Advances (ISSN 2375-2548) is published by the American Association for the Advancement of Science. 1200 New York Avenue NW, Washington, DC 20005. The title *Science Advances* is a registered trademark of AAAS.